Forty-two Color Flow Cytometry Panel Data Collected with the ID7000™ Spectral Cell Analyzer for Identifying Cellular Subsets in Human Peripheral Blood

Introduction

Multicolor flow cytometry is a high-throughput cell analysis technique that is essential for studying the biology of various cell sub-populations at a single-cell level. The peripheral immune system consists of various cellular compartments including the classical T, B, and NK cells, various innate lymphoid and myeloid subpopulations, as well as progenitor cells (Fig. 1). All these subsets are defined flow cytometrically by staining for antigens displayed on the cell surface or expressed intracellularly. One key limitation in the ability to classify the subsets had been the availability of antibody-fluorochrome combinations, as well as instrumentation's capability to distinguish the large number of individual fluorescence signals that define each subpopulation. Of late, there have been significant improvements in instrument capability, and with an increase in fluorochrome choices available to researchers, the ability to study rare subsets of cells in normal and disease states has received a significant boost.

In this study, the ID7000™ spectral cell analyzer, equipped with five lasers, has been used to define various lymphoid, myeloid, and progenitor subsets in a human peripheral blood mononuclear cell (PBMC) sample using 42 fluorescent markers.

Spectral unmixing with the ID7000 spectral cell analyzer

The ID7000 spectral cell analyzer is the highest capability cell analyzer commercially available and can be configured with up to 7 spatially separated lasers and 184 fluorescence detectors. Spectral cell analysis distinguishes the shapes of emission spectra along a large spectral range. The data is analyzed with an algorithm that replaces compensation matrices and treats autofluorescence as an independent parameter. Thus, spectral cell analysis provides improved capability to discriminate fluorochromes with similar emission peaks and provide multiparametric analysis without subjectivity (Fig. 2). Spectral analysis was developed for commercialization at Sony with the SP6800 cell analyzer that uses the Weighted Least Squares Method (WLSM) as the unmixing algorithm,[1] which has been implemented in the ID7000 system as well.

An advantage of Sony spectral analyzers is the flexibility to use any fluorescent label without specifying a detector, and the ability to distinguish very similar and widely available fluorochrome combinations such as Brilliant Violet 510 and eFluor™ 506, APC and Alexa Fluor® 647, PerCP with PerCP-Cy™5.5 and with BB700, and PE-eFluor™ 610 with Alexa Fluor® 594 and with PE-Alexa Fluor® 610 (Fig. 2B). All emission signatures, including those from the secondary lasers, are used for the intensity calculation, and use of more lasers can provide additional unmixing power.[2] When required, the ID7000 can distinguish between one or more cellular autofluorescence signatures in the same panel, and remove their contributions to other fluorochromes' calculated intensities in the unmixing process.[3] In addition, autofluorescence can be used as another marker to provide additional insights into the biology of a cell.[4]

The ID7000's automatic laser alignment, the standard high-throughput autosampler, and the standardized quality control process provide users with very consistent performance over long periods of time.[5] The automation, and availability of the Spectral Reference Library where the user can record each fluorochrome's spectral fingerprint for potential re-use at a later date, improve the efficiency and deliver cost savings to the laboratory.

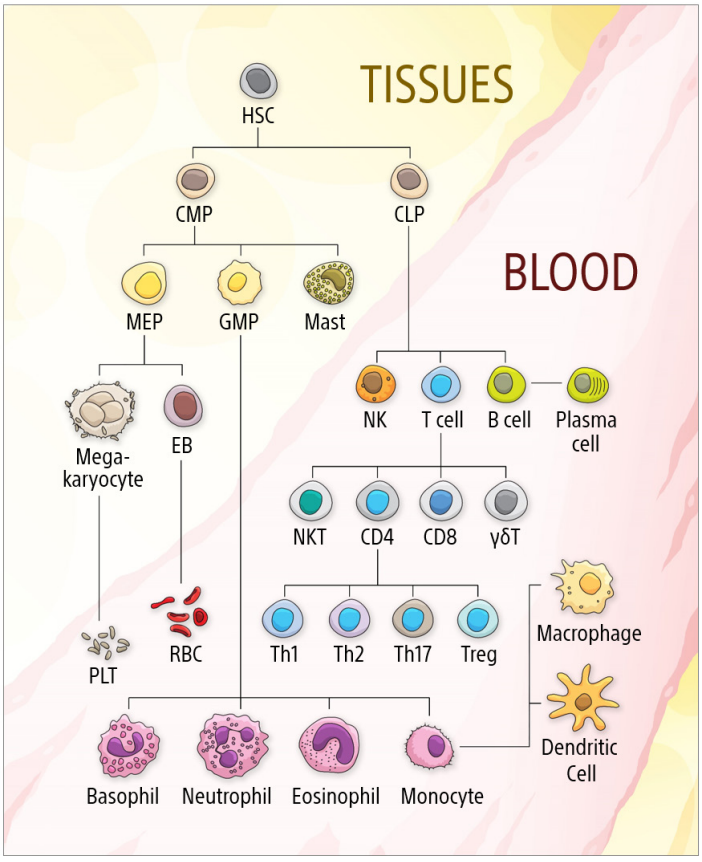

Figure 1. Major cell subsets in human blood. *Stem cells and progenitor cells in tissues such as the bone marrow, the thymus, and the lymph nodes give rise to a diverse set of innate and adaptive immune system cells as well as the non-immune populations. HSC, hematopoietic stem cell. CMP, common myeloid progenitor. CLP, common lymphoid progenitor. MEP, megakaryocytic and erythroid progenitor. GMP, granulocytic and monocytic progenitor. EB, erythroblast. PLT, platelets. RBC, red blood cells. Various CLP progeny are discussed in the results section.*

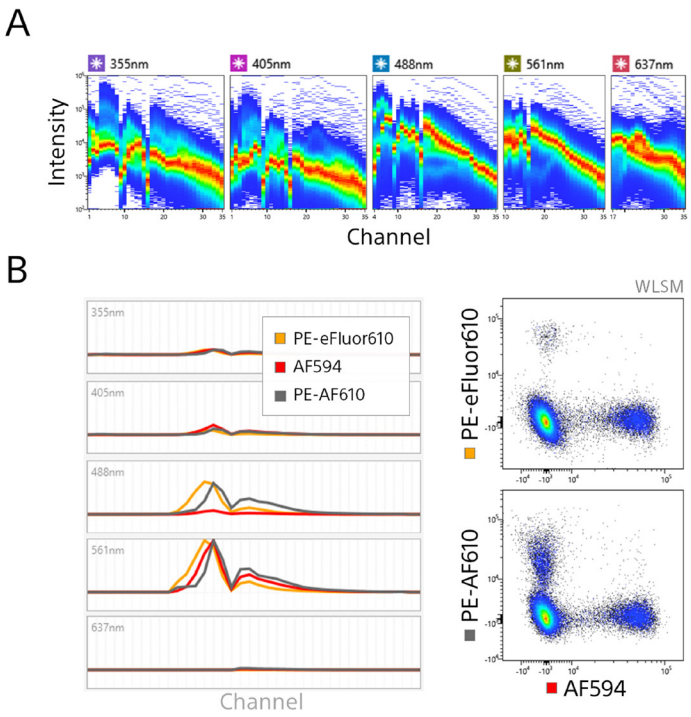

Figure 2. ID7000 spectral data examples. *(A) Spectral data collected using the ID7000 spectral cell analyzer configured with five lasers, for a freshly isolated PBMC sample stained with 42 fluorescent markers, with only red blood cells and platelets excluded via gating on Alexa Fluor® 350-negative events. Color indicates the number of cells at each intensity for each detector channel. (B) Spectral unmixing of closely overlapping fluorochromes PE-eFluor™ 610, Alexa Fluor 594®, and PE-Alexa Fluor® 610 in the 42-color PBMC sample. Single-color spectral references from the Spectral Reference Library are shown on the left, while the WLSM-unmixed data plots for all events are shown on the right. Unmixed data is similarly well resolved between PE-eFluor™ 610 and PE-Alexa Fluor® 610 (not shown).*

Gating strategy overview

Figure 3 presents a high-level summary of the gating strategy and various panels for this multicolor study. The strategy is explained in detail in the results section.

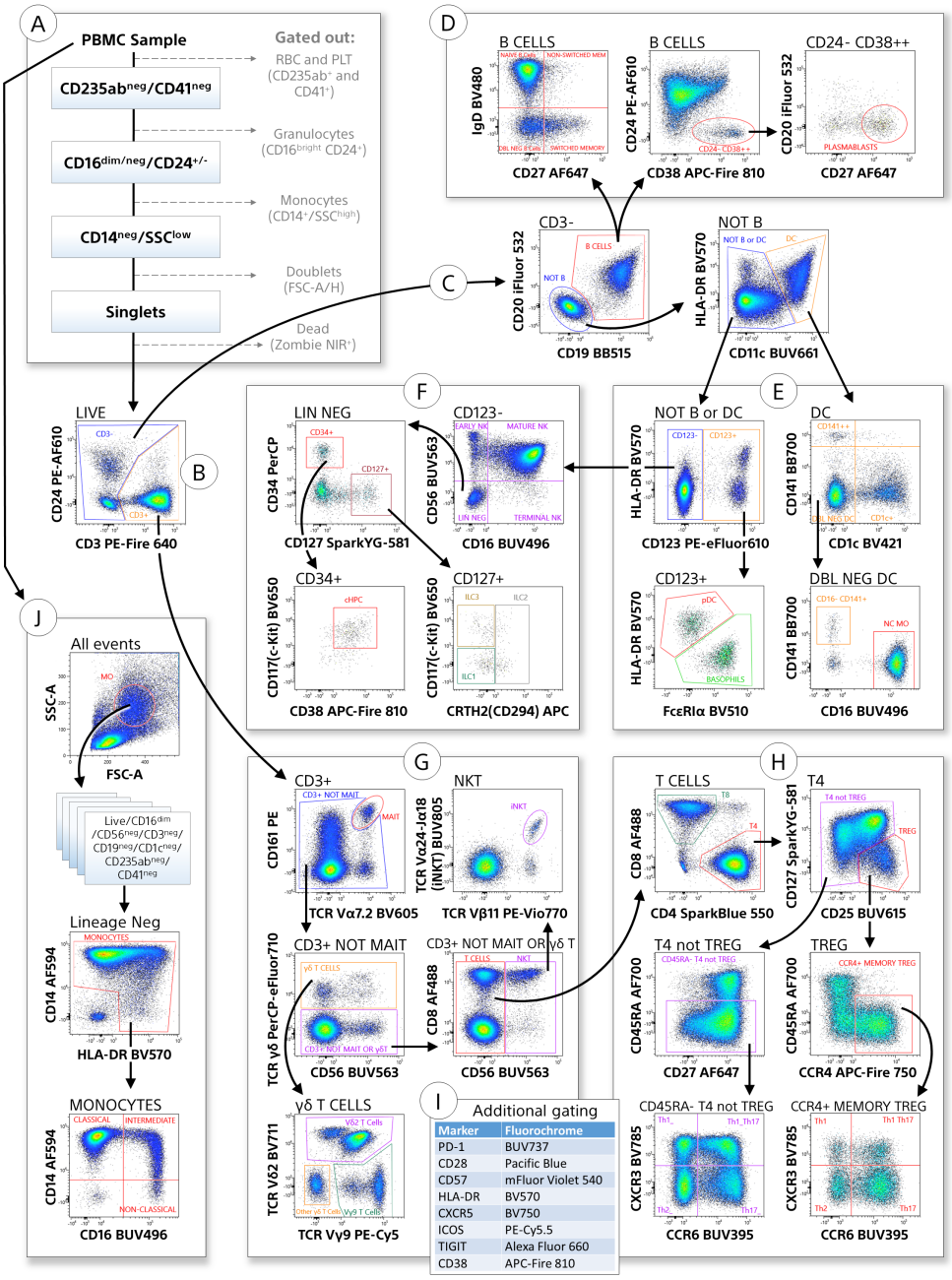

Figure 3. 42-color panel gating strategy. *(A) Pre-gating of total events. (B) CD3 gating on the live subpopulation. (C) CD3^{neg} cells gated for B and non-B subpopulations. (D) B-cell panel. (E) Dendritic cell panel. (F) NK, ILC, and progenitor panel. (G) MAIT, iNKT, and γδ T cells. (H) T-cell and Treg panel. (I) Various functional markers assessed in panels G and H (data not shown). (J) Monocyte panel.*

Order	Ex. Laser	Fluorochrome	Marker	Clone	Manufacturer	Catalog No.
1	355-nm	BUV395	CCR6/CD196	11A9	BD OptiBuild™	743356
2		-	CD235ab - Biotin	HIR2	Sony	2133090
		-	CD41 - Biotin	HIP8	Sony	2118670
		Alexa Fluor® 350	Streptavidin	-	Invitrogen (eBioscience)	S11249
3		BUV496	CD16	3G8	BD Biosciences	612945
4		BUV563	CD56	NCAM16.2	BD Biosciences	612929
5		BUV615	CD25	2A3	BD Biosciences	612997
6		BUV661	CD11c	B-ly6	BD Biosciences	612968
7		BUV737	PD-1 (CD279)	EH12.1	BD Biosciences	612792
8		BUV805	TCR Vα24-Jα18 (iNKT)	6B11	BD OptiBuild™	748828
9	405-nm	BV421	CD1c	L161	Sony	2257630
10		Pacific Blue™	CD28	CD28.2	Sony	2114640
11		BV480	IgD	IA6-2	BD Biosciences	566187
12		BV510	FcεRI	AER-37 (CRA-1)	Sony	2273130
13		mFluor™ Violet 540	CD57	HI57a	AAT Bioquest	10570120
14		BV570	HLA-DR	L243	Sony	2138190
15		BV605	TCR Vα7.2	3C10	Sony	2358600
16		BV650	CD117 (c-kit)	104D2	Sony	2166105
17		BV711	TCR Vδ2	B6	Sony	2257060
18		BV750	CXCR5 (CD185)	J252D4	Sony	2384710
19		BV785	CXCR3 (CD183)	G025H7	Sony	2368690
20	488-nm	BB515	CD19	HIB19	BD Biosciences	564456
21		Alexa Fluor® 488	CD8a	RPA-T8	BioLegend	3010247
22		Spark Blue™ 550	CD4	SK3	BioLegend	344655
23		iFluor™ 532	CD20	2H7	AAT Bioquest	10202070
24		PerCP	CD34	581	Sony	2317600
25		BB700	CD141	1A4	BD OptiBuild™	742245
26		PerCP-eFluor™ 710	TCRγδ	B1.1	Invitrogen (eBioscience)	46-9959-41
27	561-nm	PE	CD161	W18070C	BioLegend	307503
28		Spark YG™ 581	CD127 (IL-7Rα)	A019D5	BioLegend	351367
29		PE-eFluor™ 610	CD123	6H6	Invitrogen (eBioscience)	61-1239-42
30		Alexa Fluor® 594	CD14	HCD14	BioLegend	325630
31		PE-Alexa Fluor® 610	CD24	SN3	Invitrogen (eBioscience)	MHCD2422
32		PE/Fire™ 640	CD3	SK7	BioLegend	344859
33		PE-Cy™5	TCR Vγ9	B3	Sony	2256620
34		PE-Cy™5.5	ICOS (CD278)	ISA-3	Invitrogen (eBioscience)	35-9948-41
35		PE-Vio® 770	TCR Vβ11	REA559	Miltenyi (REAfinity™)	130-126-319
36	637-nm	APC	CRTH2 (CD294)	BM16	Sony	2350550
37		Alexa Fluor® 647	CD27	QA17A18	BioLegend	393205
38		Alexa Fluor® 660	TIGIT	MBSA43	Invitrogen (eBioscience)	606-9500-41
39		Alexa Fluor® 700	CD45RA	HI100	Sony	2120600
40		Zombie NIR™	Viability	-	BioLegend	423105
41		APC/Fire™ 750	CCR4 (CD194)	L291H4	BioLegend	359429
42		APC/Fire™ 810	CD38	HB-7	BioLegend	356643
		Super Bright Complete Staining Buffer		-	Invitrogen (eBioscience)	SB-4401-42
		Lymphopure™ density gradient			BioLegend	426201

Table 1. Antibody-fluorochrome and reagent list used in the technical note.

Materials and Methods

At an approved laboratory, peripheral blood mononuclear cells (PBMC) were isolated from commercially available fresh blood of a healthy donor using the Lymphopure™ solution, following all biosafety precautions. The PBMC monolayer was collected post-centrifugation and washed with a chilled bovine serum albumin (BSA)/phosphate buffered saline (PBS) staining buffer, and the cell number was quantified. Ten million cells were stained at 4°C in the dark in the presence of the Super Bright Complete Staining Buffer (eBioscience) in BSA/PBS. The panel's dyes (Table 1) were split into four groups (not indicated) for performing the staining and washing steps in sequence. BUV and BV dyes were added individually into the cell suspension to reduce the chance of unwanted polymer dye interactions. After proper incubation and washing, cells were further stained with Zombie NIR™ viability dye per the manufacturer's guidelines and with the secondary Streptavidin-Alexa Fluor® 350 conjugate. Samples were then washed, fixed with 2% formaldehyde, and resuspended in PBS buffer for data acquisition on the ID7000 spectral cell analyzer.

Unstained cells from the same donor were similarly treated and used in the data analysis steps for autofluorescence unmixing. Single-color controls were tested on both Sony antibody capture beads and the PBMC sample, with the former utilized in the unmixing matrix. Approximately 1 million events were acquired on the ID7000 at an intermediate flow rate with proper sample chilling and agitation. For reproducibility, all samples were split and acquired on two different ID7000 spectral cell analyzers on the same day. The same 42-color panel was repeated with another donor sample and run on an additional ID7000 instrument at a later date. All data analyses (spectral unmixing and gating) were performed using the ID7000 system software.

Results

To identify the lymphoid and myeloid subpopulations, red blood cells (RBC), platelets (PLT), and the majority of granulocytes and monocytes, doublets, and dead cells were first excluded by gating (Fig. 3A schematic, data not shown). Forward scatter (FSC) and CD235ab/CD41 were used to exclude small and bright positive RBC and PLT events. Granulocytes were identified and excluded as $CD16^{bright}$ and CD24 double-positive events. Next, $CD14^{+}/SSC^{high}$ monocytes were excluded. Singlets were gated based on forward scatter height and area, and dead cells excluded by gating on Zombie NIR-negative events.

Live cells were subdivided into CD3-positive and -negative subpopulations by plotting CD3 against a high-spillover channel CD24 PE-Alexa Fluor® 610 (Fig. 3B). $Live/CD3^{neg}$ cells were further gated to identify B cells using the CD19 and CD20 co-expression. IgD and CD27 expression identified Naïve and Memory B-cell subpopulations (Naïve as IgD single-positive; Non-switched memory as $IgD^{+}/CD27^{+}$; Switched memory as $IgD^{neg}/CD27^{+}$; Fig. 3D). CD24, CD38, CD20, and CD27 markers were used to identify plasmablasts ($CD24^{neg}/CD38^{bright}/CD20^{neg}/CD27^{+}$; right plots in Fig. 3D).

$Live/CD3^{neg}/CD20^{neg}/CD19^{neg}$ (NOT B) cells were gated based on HLA-DR and CD11c to identify dendritic cells (DC) ($CD11c^{+}$/HLA-DR^{+}; Fig. 3E, top plot). DCs were further subdivided into the conventional $CD141^{bright}$ (++), conventional CD1c+, and the double-negative and $CD141^{dim}$ DC (DBL NEG DC) subpopulations. From DBL NEG DC, the non-classical $CD16^{+}$ monocytes (NC MO) and the $CD16^{neg}/CD141^{dim}$ DCs were further identified (Fig. 3E, right plots). $CD16^{neg}/CD141^{dim}$ DC were also mostly $CD123^{+}$/HLA-DR^{+} (plot not shown). Additionally, $CD11c^{neg/low}$ (NOT B or DC) cells (Fig. 3E, left plots) were further subdivided into $CD123^{+}$ and $CD123^{neg}$ populations. From the $CD123^{+}$ gate, plasmacytoid DC (pDC, FcεRIα^{neg}/HLA-DR^{+}) and basophils (FcεRIα^{+}/HLA-DR^{neg}) were then identified.

The natural killer (NK) and non-NK subpopulations were identified in Figure 3E and 3F. $Live/CD3^{neg}$/ $CD20^{neg}/CD19^{neg}$/ $CD11c^{neg/low}$ cells were gated on the $CD123^{neg}$ subpopulation. Early (CD56 single-positive), mature ($CD16^{+}/CD56^{+}$) and terminal ($CD16^{+}/CD56^{neg}$) NK subpopulations were gated next (Fig. 3F, upper right plot). The non-NK, lineage negative (LIN NEG) cells were further gated based on CD34 and CD127/IL-7Rα expression, identifying the committed hematopoietic progenitor subpopulation (cHPC, $CD117^{+}/CD38^{+}$) and the noncytotoxic innate lymphoid cells (ILC1-3, $CD117^{+/-}/CRTH2^{+/-}$) (Fig. 3F, lower left and right plots, respectively).

$CD3^{+}$ T cells and their various subpopulations were identified in Figure 3G and 3H. $Live/CD3^{+}$ cells were first gated to identify the unconventional T-cell subsets (Fig. 3G). The CD161 and TCR Vα7.2 expression was used to identify the mucosal associated invariant T cells (MAIT). Non-MAIT cells were next gated for TCR γδ chains to identify various γδ T-cell subpopulations (Fig. 3G, lower plot). Non-γδ/non-MAIT $CD3^{+}$ cells were further subdivided based on CD56 expression to identify the NKT cells (Fig. 3G, middle right plot). Invariant NKT (iNKT) cells were identified as being co-positive for TCR Vα24-Jα18 and TCR Vβ11 chains (upper right plot).

Conventional T-cell subsets were identified in Figure 3H. $Live/CD3^{+}$ cells, with the unconventional subsets excluded, were gated on the CD8 (T8) and the CD4 (T4) subsets (upper left plot). CD4 T-helper cells were further distinguished as regulatory (TREG, $CD127^{low}/C25^{bright}$) and non-regulatory T cells (T4 not TREG) using CD127 (IL-7Rα) and CD25 markers. CD4 T cells and Treg cells were then gated for various T-helper subsets using CD45RA and CCR4 marker expression (middle plots). Both cell types were further subdivided into their respective memory and T-helper subsets using CXCR3 and CCR6 expression (Th1, Th2, Th1/Th17, and Th17; Fig. 3H, lower plots). The table in Figure 3I shows additional markers we utilized in assessing various cell functions (for example, activation, exhaustion, senescence) in both the conventional and unconventional T-cell subsets. Data is not shown for brevity.

Figure 3J describes monocyte gating. First, total events were gated for monocytes based on scatter and then to exclude various lineages (data not shown for brevity). Monocytes were then identified as $CD14^{+}$ and HLA-$DR^{+/-}$ (lower middle plot). Monocytes were gated for various subpopulations using CD14

and CD16 markers. A non-classical monocyte phenotype (in Fig. 3E) was also confirmed by Boolean gating (data not shown).

Discussion

Panel design considerations

The panel design considerations included marker-fluorochrome availability, dye brightness index, antigen density, and the spillover spreading matrix and the resultant cross-stain index, among others. The previously published work in the field such as OMIP-069 and other similar panels were considered as well.[6]

One of the factors affecting high parameter panel design is the spillover spreading error, because a significant number of dyes have a high degree of spectral similarity (Fig. 4, 6A and B). As a result, those dyes that are impacted by another dye's fluorescence overlap cannot be measured precisely and thus have a higher signal variance. This measurement error is revealed by the unmixing algorithm as the signal spread of the "offender" dye into the adjacent (offended) dye's parametric channel (funnel-shaped populations in Fig. 6C and Fig. 6E, top left plot). Data spread in turn may lead to a poor signal resolution between single- and double-positive biological subpopulations. To detect and avoid problematic dye combinations, the spillover spread matrix (SSM, Fig. 5) has become a commonly used tool that also guided the panel design.[7] For instance, the SSM shows that BB515 interacts with Alexa Fluor® 488, while BV480 and BV510 interact with BUV496, PE with Spark YG™ 581, and PE-eFluor™ 610 interacts with Alexa Fluor® 594.

Whereas a smaller panel would avoid these combinations, no such option often exists when working with a high-parameter panel. Therefore, one of our strategies was to assign the strongly interacting dye pairs to the well-established, mutually exclusive biological markers such as CD19 (on BB515), CD8 (on Alexa Fluor® 488), and CD4 (on Super Bright 550) (Fig. 6A, C, and E, top panel). Similarly, Alexa Fluor® 594 was assigned to the CD14 marker to identify SSC^{high} monocytes that do not express the markers on offender dyes (Fig. 6E middle plots; offenders CD123 PE-eFluor™ 610 and CD25 BUV615 not shown).

As a result of this approach, no biological double-positive populations would be expected to interfere with the downstream gating. Such an arrangement also implies that best gating may often be achieved by plotting the interacting dyes one against another, especially where a boundary between the on/off-expressed antigens is clearly distinguishable (Fig. 6C and 3B). Conversely, in cases when two lineage markers are co-expressed and do not need to be distinguished (for example, CD19 and CD20), they may be safely combined (Fig. 6D). This strategy allowed us to preserve the dyes with lower SSM values for use on markers with a more widespread expression pattern across multiple lineages and/or subpopulations.

In the context of a fully stained sample with 42 colors, a pair-wise marker resolution does not solely depend on the data spread in the positive population(s) of a given dye pair. It is equally imperative to manage the data spread of the double-negative population that arises from additional fluorochrome interactions. In Figure 6E, the lower plots describe our approach where pre-gating to exclude certain lineages leads to an improved signal resolution. As shown, B cells (red events) and other lineage populations (not colored for brevity) fall mainly in the double-negative plot area. Their fluorochromes lead to the data spread that reduces the resolution of CD56 and CD16 (NK lineage markers, left plot). As seen in the SSM (Fig. 5), the BUV496 parameter is impacted by the spreading error from BV480 (IgD) and BV510 ($Fc\varepsilon RI\alpha^+$ basophils). Gating out B cells and $CD123^+$ cells first helped us to better resolve the NK subpopulations (Fig. 6E, lower right plot).

Spectral reference adjustments

Spectral cell analysis gives user the ability to re-use single-color controls from the spectral library. The library is very similar to spectral viewers but allows us to directly apply spectral signatures to unmix the sample data. This approach is possible because Sony standardizes the PMT array performance so the detectors always achieve the same target intensity values throughout the detector range and with time.[5] Related to the PMT performance standardization, the controls are saved as proportional spectral distributions, enabling their re-use in the unmixing math.

For best practice in our 42-color panel, we recorded all the compensation bead controls on the same day and at the same voltage settings as the fully stained sample. The controls were overall of high fidelity, faithfully matching the spectra in the fully stained sample, as judged by very minimal unmixing issues (representative examples shown in Fig. 7). Of those cases, most were due to dye combinations with a high degree of spectral similarity (for example, BB515 over-unmixed out of Spark Blue™ 550, and under-unmixed out of Alexa Fluor® 488; Fig. 6A, E, top panel, and Fig. 7A and C). Other unmixing anomalies were mainly the tandem dye mismatches that resulted in a slight over-unmixing (Fig. 7A, B, and D). We made alterations to the unmixing math only sparingly, using the biology as our guide. We adjusted the over-unmixed mismatches if the sample's single-positive subpopulation clearly fell below the mean fluorescence intensity of the double-negative population in the spillover parameter (Fig. 7C). In the few under-unmixing cases, the panel was designed to keep the overlapping dyes on separate lineages. This allowed us to correct the mismatches of the reference spectra while keeping the separation indices unaffected (Fig. 7D). An additional way to handle the under-unmixing issues is by staining the fluorescence-minus-one controls, particularly in places where co-expressed markers make it difficult to adjust the unmixing matrix.

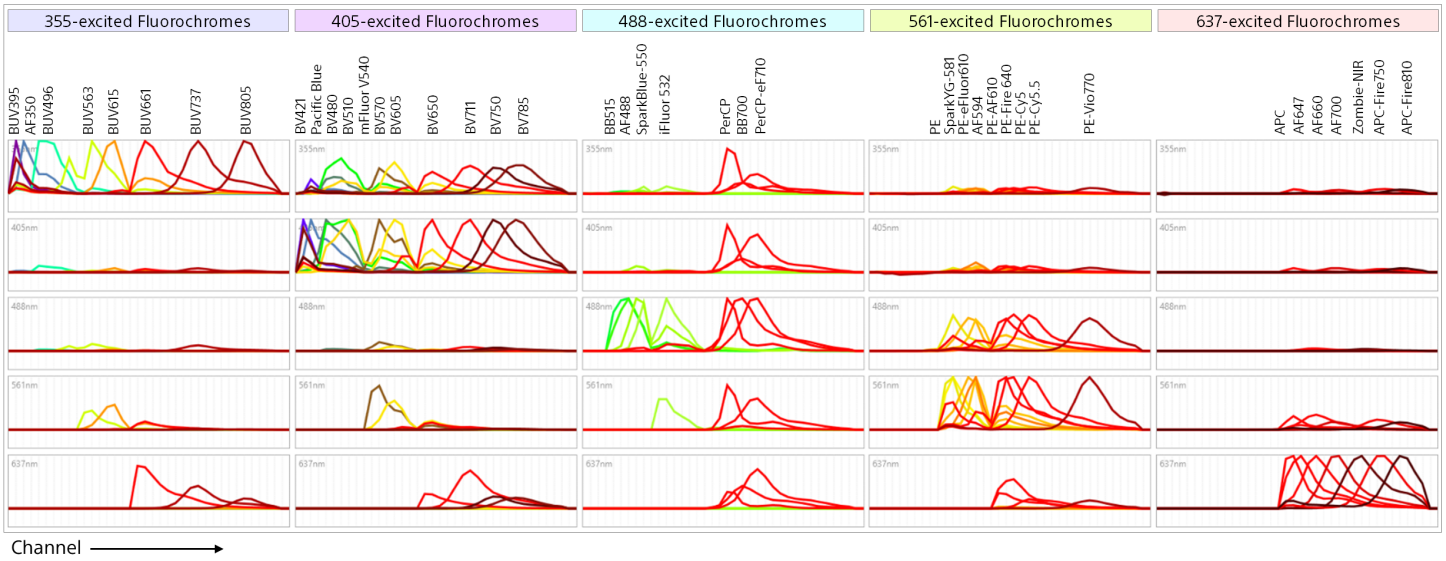

Figure 4. 42-color reference spectra from the ID7000 Spectral Reference Library. *From left to right: 355, 405, 488, 561, and 637-excited fluorochromes. All fluorochromes register their maximum emission on the expected PMT array. BUV563 and BUV615 have a small 561-excited component. BUV661 and BUV737 each have a significant 637-excited component. All 405-excited fluorochromes register minor but significant emission on the 355 PMT array. BV570 and BV605 have a significant 561-excited component. BV711 has a significant 637-excited component. iFluor™ 532 has a significant 561-excited component. PerCP is approximately equal on the 488 and 405 arrays. PerCP-eFluor™ 710 has a significant 637-excited component. PE and PE tandems have maximum emission on the 561 PMT array and minor emission on the 488 PMT array. PE/Fire™ 640 and PE-Cy™5 each have a significant 637-excited component. The 637-excited fluorochromes have very little emission on other PMT arrays.*

Offender \ Offended (SSM)	CCR6/CD196 BUV395	CD235/CD41-SA AF350	CD16 BUV496	CD56 BUV563	CD25 BUV615	CD11c BUV661	PD-1 (CD279) BUV737	TCR Vα24-Jα18 (iNKT) BUV805	CD1c BV421	CD28 PacBlue	IgD BV480	FcεRIα BV510	CD57 [mFluor Violet 540]	HLA-DR BV570	TCR Vα7.2 BV605	CD117 (c-kit) BV650	TCR Vδ2 BV711	CXCR5 (CD185) BV750	CXCR3 (CD183) BV785	CD19 BB515	CD8a AF488	CD4 SparkBlue-550	CD20 [iFluor 532]	CD34 PerCP	CD141 BB700	TCRγδ PerCP-eFluor710	CD161 PE	CD127 (IL-7Rα) [SparkYG-581]	CD123 PE-eFluor610	CD14 AF594	CD24 PE-AF610	CD3 [PE-Fire 640]	TCR Vγ9 PE-Cy5	ICOS (CD278) PE-Cy5.5	TCR Vβ11 PE-Vio770	CRTH2 (CD294) APC	CD27 AF647	TIGIT [AF660]	CD45RA AF700	Viability Zombie-NIR	CCR4 (CD194) APC-Fire750	CD38 [APC-Fire810]
CCR6/CD196 BUV395		9	4	1	1	0	1	0	0	0	3	5	3	0	0	0	0	0	0	1	1	0	0	0	0	0	0	0	0	0	0	0	0	0	0	0	0	0	0	0	0	0
CD235/CD41-SA AF350	7		16	1	1	0	1	0	1	1	3	7	5	0	0	0	0	0	0	1	1	0	0	0	0	0	0	0	0	0	0	0	0	0	0	0	0	0	0	0	0	0
CD16 BUV496	3	3		6	4	2	3	1	1	1	6	27	19	3	1	1	0	1	1	14	15	5	4	1	0	1	3	2	1	2	1	1	1	0	0	1	0	0	0	1	0	0
CD56 BUV563	8	3	2		6	2	1	2	0	0	1	3	3	2	1	0	0	0	0	3	4	4	17	1	1	1	11	34	5	4	4	2	1	1	0	2	1	1	0	0	0	0
CD25 BUV615	6	2	2	2		5	2	2	0	0	2	3	2	1	4	2	1	1	0	1	1	1	1	2	3	1	2	7	5	61	5	3	3	2	0	4	2	1	1	1	0	0
CD11c BUV661	7	3	3	1	2		6	3	1	0	3	5	4	0	1	4	2	1	1	2	2	1	1	3	5	2	2	1	1	2	2	4	5	6	1	50	32	16	7	4	3	3
PD-1 (CD279) BUV737	0	3	3	1	1	1		6	0	0	2	4	3	0	0	0	0	2	3	1	1	1	1	1	2	8	1	0	0	0	0	1	1	3	2	2	2	3	8	12	6	3
TCR Vα24-Jα18 (iNKT) BUV805	21	7	7	2	1	1	2		1	1	6	11	7	1	0	0	0	1	1	2	2	1	1	0	0	0	1	0	0	1	0	0	1	0	0	1	1	1	1	2	4	5
CD1c BV421	0	58	15	2	1	0	0	0		7	11	20	13	2	1	0	0	0	0	2	1	0	0	0	0	0	1	1	0	0	0	0	0	0	0	0	0	0	0	0	0	0
CD28 PacBlue	0	16	24	3	1	0	1	0	7		15	28	19	3	1	1	0	1	1	3	2	0	1	0	0	0	1	2	0	0	0	0	1	0	0	0	1	1	0	0	0	0	0
IgD BV480	0	2	73	7	3	1	2	1	2	3		51	38	6	3	1	1	2	1	16	17	6	6	1	0	0	5	3	1	2	1	1	1	0	0	1	0	0	0	0	0	0
FcεRIα BV510	0	3	64	18	5	3	2	1	2	2	35		45	7	5	2	1	2	1	5	4	2	3	1	1	0	3	6	1	3	1	1	1	0	0	2	1	1	1	1	0	0
CD57 [mFluor Violet 540]	0	4	29	29	4	2	2	1	1	1	23	49		8	5	2	1	2	1	5	6	3	4	1	1	0	4	6	2	3	2	1	1	0	0	2	1	1	1	0	0	0
HLA-DR BV570	0	1	6	12	14	3	1	1	4	3	9	14	10		9	3	1	1	1	3	3	2	4	3	2	1	15	30	6	8	6	5	4	2	0	2	1	1	1	0	0	0
TCR Vα7.2 BV605	0	2	4	3	50	7	3	2	3	2	5	8	5	4		7	3	3	2	2	2	1	1	5	3	2	4	11	13	31	9	7	7	3	1	5	2	2	2	1	1	0
CD117 (c-kit) BV650	0	1	4	1	7	46	4	2	4	2	5	9	6	2	3		4	3	2	2	3	1	2	4	4	2	2	2	2	5	3	5	6	3	1	27	14	8	4	2	2	1
TCR Vδ2 BV711	0	1	5	1	0	2	32	5	6	2	6	11	7	1	1	1		13	5	2	1	0	0	3	7	8	3	1	1	1	1	2	2	8	1	5	9	12	10	6	5	3
CXCR5 (CD185) BV750	0	0	6	2	1	1	23	10	6	2	8	14	9	2	1	1	3		6	3	3	1	1	1	2	3	1	1	1	0	1	1	1	1	2	2	2	3	4	8	5	3
CXCR3 (CD183) BV785	0	5	8	2	1	1	6	33	22	4	10	18	12	2	1	1	2	6		4	5	2	2	1	1	1	2	1	1	1	1	1	1	1	2	2	2	2	3	5	7	5
CD19 BB515	0	1	14	2	1	0	1	0	0	0	4	10	10	2	1	0	0	0	0		87	25	18	0	1	1	7	2	3	3	2	1	1	1	0	1	0	1	0	0	0	0
CD8a AF488	0	0	4	1	0	0	0	0	0	0	2	5	5	1	0	0	0	0	0	31		12	9	0	1	1	3	1	1	2	1	0	0	0	0	0	0	0	0	0	0	0
CD4 SparkBlue-550	0	0	6	5	1	1	0	0	1	1	7	21	26	4	2	1	0	0	0	12	18		15	1	1	1	9	4	3	4	2	1	1	1	0	1	0	1	0	0	0	0
CD20 [iFluor 532]	0	1	1	24	2	1	0	1	0	0	2	5	5	2	1	1	0	0	0	6	8	9		1	2	1	18	38	8	6	6	3	2	1	0	1	1	1	0	0	0	0
CD34 PerCP	0	0	0	0	0	4	4	1	0	0	0	0	0	0	0	2	3	3	2	1	2	1	1		6	6	2	0	1	1	2	5	9	4	1	8	11	6	4	3	2	1
CD141 BB700	0	1	3	3	2	7	11	3	3	0	4	9	11	3	2	4	11	7	4	12	17	9	10	10		14	7	3	4	6	4	4	7	11	3	15	18	21	11	8	8	4
TCRγδ PerCP-eFluor710	0	2	0	0	0	2	26	3	6	0	0	0	1	0	0	1	22	10	3	1	2	1	1	6	16		7	3	2	2	1	2	3	20	3	5	7	9	18	7	5	3
CD161 PE	0	0	1	6	6	1	0	0	1	0	2	2	1	8	2	1	0	0	0	3	4	3	5	1	1	1		91	16	6	10	5	2	1	0	1	1	1	0	0	0	0
CD127 (IL-7Rα) [SparkYG-581]	0	0	1	2	2	0	0	0	0	0	1	1	1	3	1	0	0	0	0	1	1	1	1	1	1	1	15		6	4	4	3	2	1	0	1	1	1	0	0	0	0
CD123 PE-eFluor610	0	2	1	2	22	2	1	0	1	0	1	1	1	1	8	2	1	0	0	4	4	2	2	2	5	2	13	48		87	26	8	4	4	1	2	2	2	1	0	0	0
CD14 AF594	0	0	0	1	16	4	1	1	1	0	0	1	1	1	6	3	1	1	0	1	1	1	1	3	3	2	3	4	7		9	6	5	3	1	5	3	2	1	1	1	0
CD24 PE-AF610	0	1	1	1	10	11	1	1	1	0	0	1	1	1	4	5	2	1	0	3	4	2	2	4	10	5	8	5	23	80		20	10	7	1	10	5	5	2	1	1	0
CD3 [PE-Fire 640]	0	1	1	1	2	17	2	1	2	0	0	1	1	1	1	7	5	1	1	4	5	3	2	6	24	8	5	4	5	22	17		15	17	1	22	13	13	5	3	2	1
TCR Vγ9 PE-Cy5	0	1	1	1	1	23	2	1	2	0	1	1	2	1	1	4	8	1	1	2	4	3	2	11	44	7	9	3	3	3	4	10		23	2	34	41	30	11	5	2	1
ICOS (CD278) PE-Cy5.5	0	1	1	3	1	3	10	1	4	0	1	2	2	3	1	1	15	2	1	3	5	5	3	8	52	25	35	29	4	8	5	4	6		3	3	4	17	4	3	2	1
TCR Vβ11 PE-Vio770	0	0	2	1	0	0	2	4	1	0	0	0	0	1	1	0	1	2	2	6	8	4	5	1	2	3	6	5	3	3	3	2	2	2		2	3	2	3	5	6	4
CRTH2 (CD294) APC	0	0	0	0	1	14	2	1	0	0	0	0	0	0	1	3	1	1	1	1	1	0	1	3	4	1	2	1	1	1	2	4	5	4	1		29	12	6	3	3	2
CD27 AF647	0	0	0	0	0	2	1	0	0	0	0	0	0	0	0	1	1	0	0	1	1	1	1	1	3	1	1	0	0	0	1	2	2	3	0	16		11	6	2	2	2
TIGIT [AF660]	0	0	1	0	0	3	3	1	1	0	0	1	1	0	0	1	3	1	1	2	3	1	1	3	16	3	6	3	2	1	1	2	3	17	1	8	12		8	4	4	2
CD45RA AF700	0	0	0	0	0	1	10	2	1	0	0	0	0	0	0	0	4	3	2	3	4	2	2	1	5	3	3	1	1	1	1	1	1	7	1	4	7	8		7	6	4
Viability Zombie-NIR	0	1	9	3	2	1	7	5	2	1	10	19	13	3	2	1	3	6	4	10	13	6	6	2	4	7	5	3	2	2	2	3	3	5	7	8	10	10	16		24	17
CCR4 (CD194) APC-Fire750	0	1	1	0	0	1	1	9	1	0	1	2	1	0	0	0	0	1	3	1	1	0	0	1	1	1	0	0	0	1	1	1	1	1	3	5	4	3	3	7		7
CD38 [APC-Fire810]	0	2	0	0	0	2	1	11	1	0	0	0	0	0	0	1	1	1	2	0	0	0	0	1	2	1	1	0	0	1	1	2	2	2	1	9	7	4	3	3	6	

Figure 5. Spillover Spreading Matrix for the 42-color Sony ID7000 immunophenotyping panel. Data from the single-color controls on antibody-capture beads was used to calculate the SSM following a published method.[7] Each cell value quantitates the amount of spillover spreading error that a primary color's fluorescence signature (each row; offender dye) creates in the unmixed "spillover" parameter channel (each column; offended dye). Each SSM value depends on the magnitute of spectral similarity of the dye pair and the instrument setup (voltage, detector sensitivity, etc.), but it is independent of the fluorochrome intensity. Values are not directly comparable with other cytometers. Together with fluorochrome brightness index and a known antigen density, SSM is a tool that aids with proper panel design and data gating. Marker names indicated in blue.

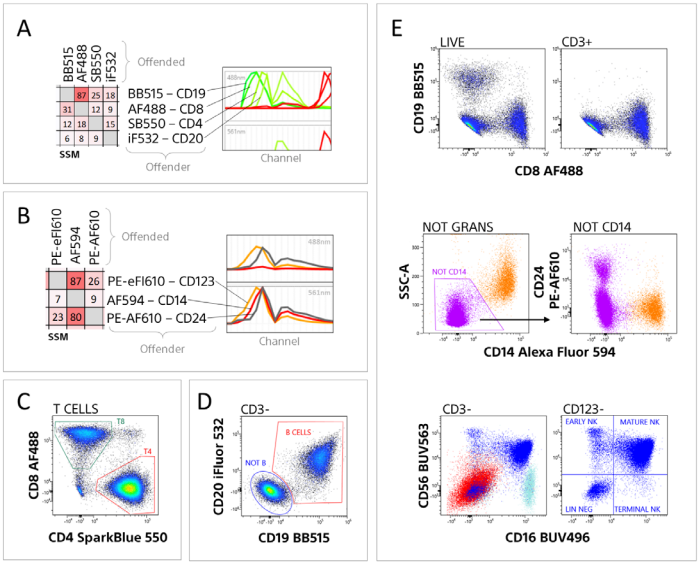

Figure 6. Panel design and gating examples. *(A) SSM spreading error values (left) and the corresponding emission signatures from the spectral library on the 488-nm PMT array (right) are shown, with BB515 and Alexa Fluor® 488 (AF488) having a high degree of spectral overlap. SB550, Spark Blue 550. iF532, iFluor 532. Rows indicate the primary offender fluorochromes. Columns indicate the offended dyes. (B) Data for the indicated three fluorochromes is shown, in a similar format to Panel A. Alexa Fluor® 594 (AF594, red curve) is significantly "offended" by both PE-eFluor™ 610 (PE-eF610) and PE-Alexa Fluor® 610 (PE-AF610), but not vice-versa. (C) Spectral overlap between Alexa Fluor® 488 and Spark Blue 550 results in the data spread of single-positive subpopulations (funnel-shaped gates). Assigning each dye to the biological single-positive subpopulations avoids the need to gate on the double-positive subpopulation. (D) B cells were identified as double-positive for CD19 and CD20, both assigned to fluorochromes described in Panel A. (E) Gating approaches. Top plots: Data spread between CD19-BB515 and CD8-AF488 (left plot) is managed by gating on the CD3⁺ subpopulation first (right plot). Middle plots: SSC-A^{high}/ CD14⁺ monocytes were assigned to Alexa Fluor® 594, a dye that interacts with CD24 PE-Alexa Fluor® 610 (B-cell lineage marker). Gating out monocytes therefore excludes them from subsequent analysis. Bottom panel: Left dot plot of total CD3^{neg} cells contains B cells (from Panel D, in red) and other cell types (Live gate in light blue). Their removal by pre-gating (not shown) helps to distinguish NK subpopulations (right plot, dark blue).*

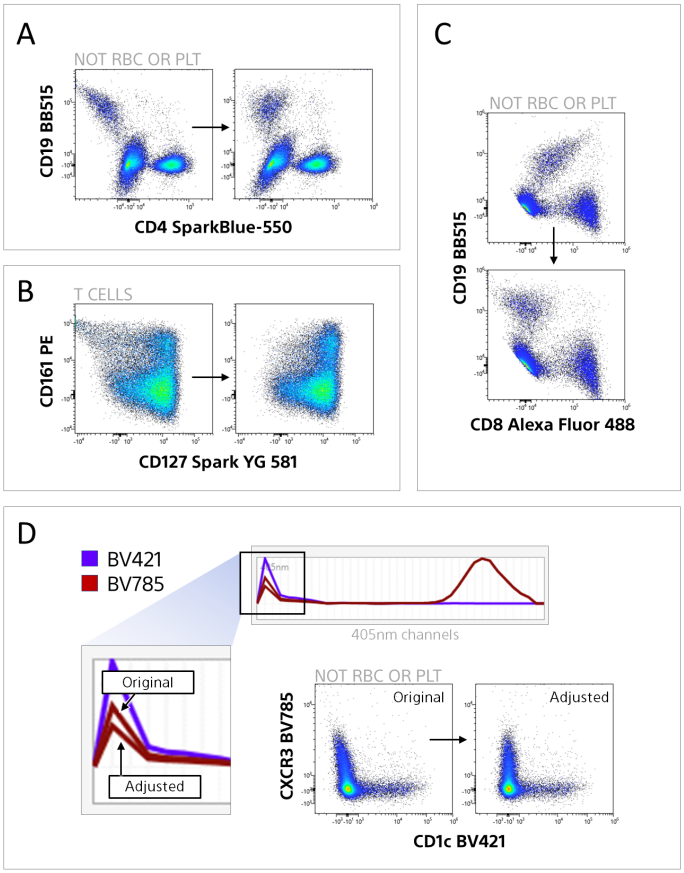

Figure 7. Spectral unmixing adjustments. *Representative examples of the mismatches between the reference spectra of single-color controls and the fully stained sample are shown. RBC- and PLT-excluded events are shown, except panel B. (A-B) Representative examples of over-unmixed data. Adjustments were made to the biologically single-positive subpopulations falling below the mean fluorescence intensity of the double-negative subpopulation in the spillover channel (x-axis). (C) Representative example of the under-unmixed data. Adjustments were made because the biologically double-positive subpopulation was not expected to exist. (D) A BV785 tandem dye mismatch resulted in its over-unmixing from the BV421 channel. The spectral library and the inset box show the result of adjustments where the "donor" component of the BV785 spectral curve was reduced, leading to the corrected parametric data (right plot).*

Conclusions

In this study, our considerations were to determine the best fluorochrome set to use for 40- to 45-color panels on the ID7000. We aimed to incorporate a set of core markers that utilize the most challenging fluorochrome combinations while leaving the less challenging fluorochromes available for substitutions by users to make derivative panels. We used tools such as the Spectral Reference Library and the Spillover Spreading Matrix to test for ideal fluorochrome combinations, with at least three more dyes ready to expand the panel size with this five-laser instrument configuration. We also optimized our panel design and gating methods to enable good marker/fluorochrome choices in the future.

Acknowledgment

The authors would very much like to thank Patricia Rogers at the Broad Institute Flow Cytometry Core for her unwavering support of this work.

References

1. Futamura K, Sekino M, Hata A, et al. Novel full-spectral flow cytometry with multiple spectrally-adjacent fluorescent proteins and fluorochromes and visualization of in vivo cellular movement. *Cytometry A.* 2015;87A:830-842.

2. Futamura K, et al. Technical Note: Increasing Panel Design Flexibility Using the 320-nm Laser on the ID7000™ Spectral Cell Analyzer. Sony Corporation. CYTO poster #150 (2021).

3. Nao Nitta, PhD, Greg Veltri, PhD, Mark Dessing. Method and Theory of the Autofluorescence Unmixing in Spectral Cell Analyzers. Sony Corporation. Technical Bulletin (2016).

4. Peixoto MM, Soares-da-Silva F, Schmutz S, et al. Identification of fetal liver stromal subsets in spectral cytometry using the parameter autofluorescence. Article in review. *BioRxiv.* 2021. https://doi.org/10.1101/2021.09.29.462345

5. Miyata, et al. Advanced Flow Cytometry Standardization with the ID7000™ Spectral Cell Analyzer. Sony Corporation. CYTO poster #149 (2021).

6. Parker LM, Lannigan J, Jaimes MC, et al. OMIP-069: Forty-color full spectrum flow cytometry panel for deep immunophenotyping of major cell subsets in human peripheral blood. *Cytometry A.* 2020;97A:1044-1051.

7. Nguyen R, Perfetto S, Mahnke YD, Chattopadhyay P, Roederer M. Quantifying spillover spreading for comparing instrument performance and aiding in multicolor panel design. *Cytometry A.* 2013;83:306-315.